AIMS Materials Science, 5(6): 1102–1111.
DOI: 10.3934/matersci.2018.6.1102
Received: 27 August 2018
Accepted: 08 November 2018
Published: 12 November 2018

http://www.aimspress.com/journal/Materials

Research article

The coated porous polyimide layers for optical scattering films

Hyeck Go[1,2], Eun-Mi Han[2], Moon Hee Kang[1,3], Yong Hyun Kim[4] and Changhun Yun[1,*]

[1] Center for Nano-Photonics Convergence Technology, Korea Institute of Industrial Technology (KITECH), Gwangju, 61012, Korea
[2] School of Chemical Engineering, Chonnam National University Gwangju, 61186, Korea
[3] Department of Electrical Energy Engineering, Keimyung University, Daegu, 42601, Korea
[4] Department of Display Engineering, Pukyong National University, Busan, 48513, Korea

* **Correspondence:** Email: chyun@kitech.re.kr; Tel: +82626006540; Fax: +82626006509.

Abstract: We have investigated the optical scattering characteristic of the air-void micro-structure of air-voids of the porous polyimide (PI) layer prepared from a simple polyimide-precursor coating and the immersion precipitation method. For the careful control or tune of the generated pore-structure, the content of polar aprotic solvent in polar protic non-solvent bath was adjusted during the pore-generation process. To account the correlation between the generated micro-structure of a porous polymer layer and its optical scattering property, the optical haze values were calculated and compared with the measured total transmittance and diffuse transmittance values. And the calculated average optical haze value decreased from 0.88 to 0.53 as increasing the content of polar aprotic solvent in the coagulation bath. In addition, the light scattering mechanism was proposed for a prepared porous polymer film consisting of air-voids inside the polymer media and the rough surface at the ambient interface. Finally, for an analytical explanation, we also introduced Mie scattering and Scalar surface scattering which explains the light scattering inside pore structure as well as at the rough surface, respectively. Based on our systematic approach, it can be said that the net power of light scattering was the sum of Mie scattering and the surface scattering.

Keywords: porous polymer layer; optical scattering; haze film; immersion precipitation; polyimide

1. Introduction

The optical scattering phenomena have been widely applied on the conventional optics or optoelectronic devices, such as general solid state lightings, photovoltaic panel, smart windows, and

displays [1–5]. Normally, conventional light scattering layer is consisted of high-index nano- or micro- particles on the surface or inside the polymer media, which act as a random optical interaction media of different composites with different refractive indexes [1,2,4]. Resulting from changes of light path through a medium which contains over two different materials, the collective rays from those light scattering films provide the uniform angular distribution in both optical power and luminescent spectrum [2,6]. Recently, an alternative optical scattering layer based on the porous structure has been studied from many research groups; these porous layers utilize the index contrast between the media material and the air void [7–9]. Compared with the conventional light scattering layers, the porous scattering layer can have advantages in terms of enhanced uniformity of power distribution and color stability, because air voids do not have in-situ absorption and the index contrast between an air void and a media material is relatively high. Moreover, a porous polymer layer has attracted lots of interest due to rising demand for manufacturing cost reduction. Koh et al. reported the porous polymer scattering layer via high index contrast between polyimide (Kapton with $n \sim 1.7$) and air voids ($n \sim 1.0$) [10]. In this research, using a simple coating process and the immersion precipitation method, uniform and scalable porous scattering films were prepared and introduced to OLEDs. We also have reported that porous polyimide scattering layers without any frustrating laminating process, where a proper choice of a polar aprotic solvent during immersion pore-generation process allowed us to prepare porous micro-structures with uniform pore-size and controlled pore-shape [11]. Although there have been reported various benefits and potential significance of porous polymer scattering layers, but only few theoretical approach has been performed to account their porous micro-structures with their optical scattering characteristics.

The present study explores a novel and original method to realize fine control or tuning of the optical scattering characteristic of porous polyimide film for the first time. To prepare porous polyimide layers, we utilized immersion precipitation method from the coated poly amic acid layer. The optical scattering properties can be controlled by adjusting contents of polar aprotic solvent in polar protic non-solvent bath during the pore-generation process. In particular, we focused on the impact of generated micro-structure of air voids in the porous polyimide layers to their optical scattering characteristics. In addition, by introducing Mie scattering theory and Scalar surface scattering theory, a systematic approach has been performed to explain the influence of the micro-structures inside the prepared porous polymer layer.

2. Materials and method

Fabricating a poly imide (PI) film can be done from two kinds of synthetic routes: (i) the thermal imidization process after coating the corresponding poly amic acid (PAA) precursor layer, (ii) the evaporation of solvents from the directly-coated poly imide layer. In this research the porous PI film was made from the imidization process with coated PAA layer, because the solution of PAA precursor has good compatibility with the immersion precipitation method [11–13]. To prepare PAA precursor for the porous colorless PI film, we started from dissolving 4,4'-oxydiphthalic anhydride (>98% TCI Korea, Figure 1a) and 2,2-bis[4-(4-aminophenoxy)phenyl] hexafluoropropane (>98% TCI Korea, Figure 1b) in a polar aprotic solvent, N,N-dimethylacetamide (DMAc, 99.8% anhydrous Alfa Aesar). Then, both solutions were mixed at a molar ratio of 1:1 and kept the mixture solution stirring for 24 hours in an N_2-filled glove box to prevent the moisture quenching. The synthesized yellowish PAA precursor (Figure 1c) solution was diluted to 3.5 wt% using DMAc and kept in glove

box before the following coating process. Before coating the PAA solution, thin zinc oxide (ZnO) layers as an adhesion-promoting layer was coated onto the glass substrates; these layers were converted from Zn acetate (Alfa Aesar) in ethanolamine (Sigma-Aldrich) by baking a coated sample at 200 ºC on a hot plate for 1 hour in air ambient [14]. This 5-nm-thickness ZnO buffer enhances the coating uniformity and prevents the porous PAA precursor from floating in the non-solvent bath during the immersion precipitation process. The PAA layer was spin-coated at 1000 rpm for 30 s on a ZnO-coated glass substrate and then submerged into non-solvent bath for 2 min; where the clear coated PAA layer turned into the diffuse porous PAA film. To control the micro-structure inside the porous PAA layer, we changed the contents of DMAc solvent in the Deionized water (DIW) bath at 0 vol%, 16 vol%, 32 vol%, and 48 vol%. After blowing out the remaining solvents, the prepared porous PAAs on glass substrates were placed in a convection oven at 170 ºC for 30 min to dry resultant DMAc solvent. Finally, the porous PAA layers were changed into porous PI layers (Figure 1d) through thermal imidization reaction by putting substrates on a 310 ºC hot plate for 5 min.

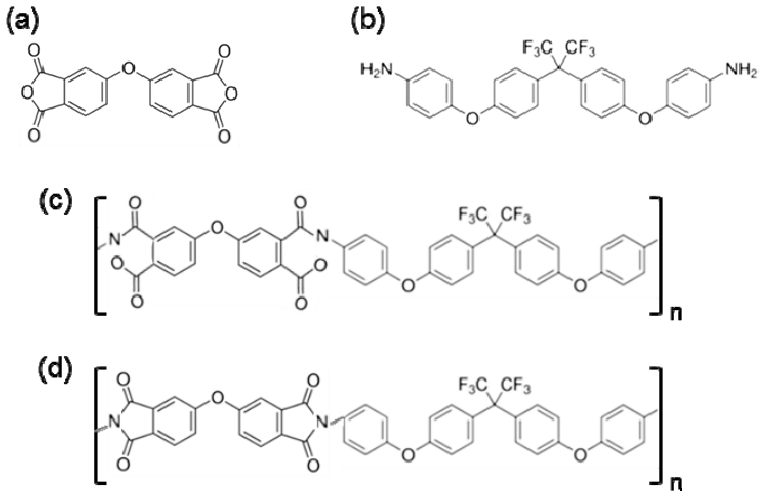

Figure 1. The chemical structures of (a) 4,4'-oxydiphthalic anhydride; (b) 2,2-bis[4-(4-aminophenoxy)phenyl] hexafluoropropane as the starting materials; (c) the synthesized poly amic acid precursor; and (d) the colorless polyimide from the thermal imidization process of c.

The cross sectional SEM images and the surface roughness values for generated porous PI films were analyzed through the SEM(SU8230, Hitachi) and AFM(Park-XE15, Park Systems) measurements, respectively. The optical properties of the prepared porous PI layers were measured using a spectrophotometer with an integrating sphere (CM-3700d, Konica, Minolta) and a UV-Vis spectrometer (Cary 5000, Agilent).

3. Results and discussion

3.1. The micro-structure of porous polyimide films

As previously reported, the micro-structure of pores in porous polymer layers determines their

optical or mechanical properties [7–9]. In this work, the immersion precipitation method was utilized to make the porous polymer film. For the systematic study regarding the influence of generated micro-structure of air voids in the porous polyimide (PI) layers on the optical scattering properties, we first controlled the pore-generation process by changing the condition of coagulation bath. Through the immersion precipitation process using deionized water (DIW) baths with different contents of N,N-dimethylacetamide (DMAc), different micro-structures were generated. The images in Figure 2 represent cross sectional SEM images of porous polyimide films through pore-generation in different coagulation bath. As can be seen in Figure 2, the resultant pore structure shows big difference depending on the composition of coagulation bath. With the increased DMAc solvent content in the DIW non-solvent bath, the number and size of the air voids were reduced and the cellular shape started to be dominant. Similar with our previous reports, the sample from only DIW coagulation bath has various sizes of pores from few hundred nano-meters to micro-meters (Figure 2a), and the total thickness of porous layer was measured around 7 μm. However, for the sample with DMAc solvent of 16 vol%, 32 vol%, and 48 vol% in DIW bath, the thickness was 5.5 μm, 4.0 μm, and 3.5 μm. The thickness-decrease in samples with various DMAc contents comes from the reduction of amount of air voids inside. As the contents of DMAc in DIW bath increased, the pore-size decreased to below a few hundred nano-meters. From the analysis of cross sectional SEM images, one may conclude that the generated pore-structure of porous PI layers was controlled from the contents of DMAc solvent in the DIW bath.

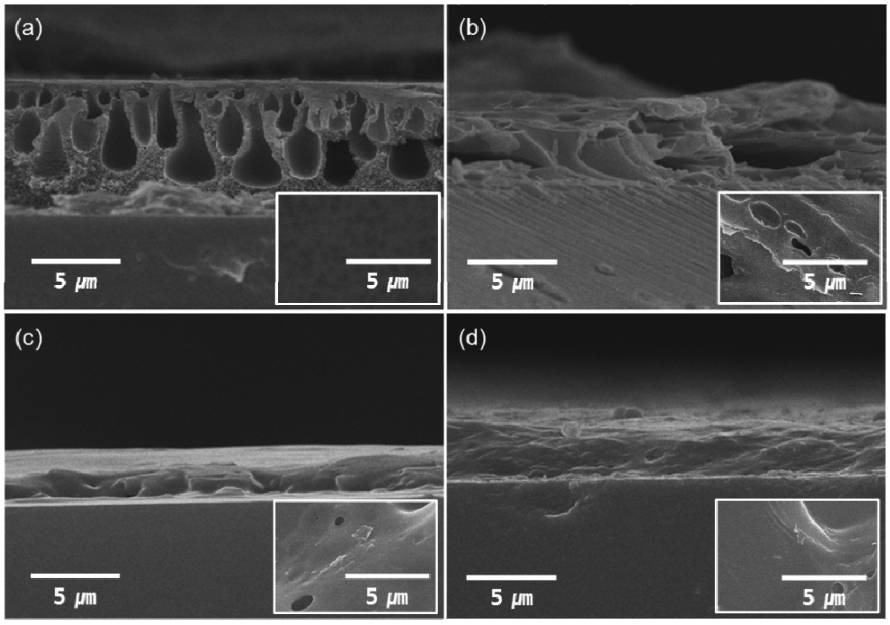

Figure 2. Cross sectional SEM images of porous polyimide films prepared through the immersion precipitation method using water bath with different contents of N,N-dimethylacetamide (DMAc) of (a) 0 vol%, (b) 16 vol%, (c) 32 vol%, and (d) 48 vol%. Insets are the corresponding top-down SEM images.

To check the influence of the generated pore-structure in porous PI layers on their surface roughness, AFM images were taken and compared. As shown in Figure 3, the surface roughness can also be distinguished depending on the composition of coagulation bath during pore-generation

process. In the sample with only DIW bath, a flat surface with an average roughness of 3.1 nm and the peak-to-valley roughness of 37 nm were obtained (Figure 3a). And the measured values of the average roughness (the peak-to-valley roughness) were 45 nm (316 nm), 56 nm (451 nm) and 98 nm (722 nm) for the 16 vol%-, 32 vol%- and 48 vol%-porous PI samples, respectively. From the surface roughness of porous PI layers, the generated micro-structure at the surface can also be tuned by the coagulation bath conditions.

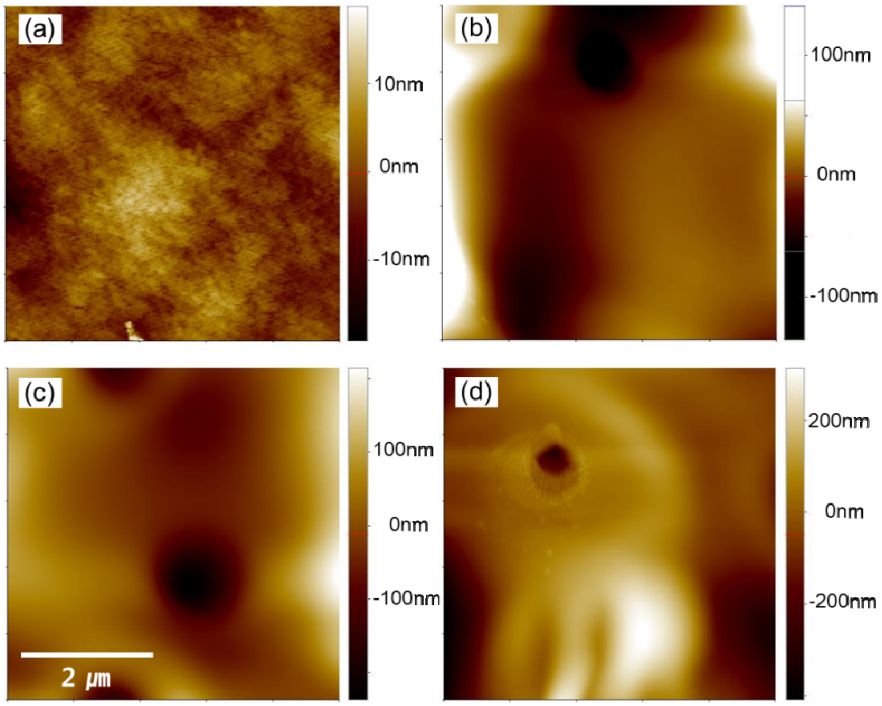

Figure 3. Measured AFM images of porous polyimide films prepared through the immersion precipitation method using water bath with different contents of N,N-dimethylacetamide (DMAc) of (a) 0 vol%, (b) 16 vol%, (c) 32 vol%, and (d) 48 vol%, where the scan size was fixed at 5 μm × 5 μm.

The difference of micro-structure between the prepared porous PIs can be explained by the pore-generation mechanism depending on the condition of coagulation bath. Based on the previous report, the addition of solvent to a coagulation bath during the immersion precipitation method can affect the exchange rates of the DMAc solvent in the coated poly amic acid (PAA) layer and the mixed non-solvent in the coagulation bath [11–13]. The higher concentration of solvent in DIW bath provided the lower inflow of DIW non-solvent into the coated PAA layer. Resulting from the slow exchange rate, the mixed PAA layer can stay longer in metastable region [15]. During the first period right after coated PAA layer immersion, the initial film thickness hardly decreases. However, the PAA polymer concentration near the interfacial boundary increases strongly at the moment of contact between the polymer solution and the mixed bath [16,17]. Resulting from the sudden increase of polymer concentration, there are two possible phase separation routes; a spinodal decomposition and a nucleation and growth. In DIW bath, the interfacial boundary separated into a polymer-rich and a polymer-poor phases via a spinodal decomposition due to the fast exchange rate [15,17]. The inflow of DIW non-solvent beneath the interfacial skin layer mainly happens through a polymer-poor region

rather than a polymer-rich region. Thus, the phase separation inside the coated PAA layer can show the formation of channeling morphology through PAA-poor phases by successive spinodal decompositions [15]. From this reason, the porous PI films with a large pore-size and a flat surface was generated after the pore-generation in DIW bath. However, based on SEM images in Figure 2, it can be estimated that the dominant phase separation shifted from a spinodal decomposition to a nucleation and growth in coagulation bath with high solvent content. Due to the slow exchange rate of mixed non-solvent, membrane can be formed through the metastable region. Resulting from the continuous exchange until the onset of a phase separation, the region of highly concentrated PAA solution beneath the interface increases considerably [15–17]. From this reason, the PAA polymer concentration of this intermediate layer is high, and the phase separation occurs from a nucleation and growth. Consequently, the chance for the formation of channeling morphology is small and the porosity induced from this mechanism could be relatively low. Also, the rough surface of the generated porous layer can be explained because the intermediate layer can influence the mass transport behavior, resulting in the higher chance to form a porous structure at the interface between the bath and the coated layer [15].

3.2. The optical scattering properties of porous polyimide films

To confirm the influence of the generated pore-structure of the prepared porous PI layers on their optical properties, we performed the optical scattering measurement for porous samples with different contents of DMAc solvent in DIW non-solvent bath. First, total (T_T (λ)) and diffuse transmittance spectra (T_D (λ)) were obtained using a spectrophotometer with an integrating sphere (Figure 4a, b). T_T (λ)s had a slight difference depending on the condition of coagulation bath, where the average total transmittance ($T_{T,avg}$) values were 77%, 81%, 83% and 84% for samples with DMAc solvent of 0 vol%, 16 vol%, 32 vol%, and 48 vol%, respectively. However, the diffuse transmittance varied noticeably; average diffuse transmittance ($T_{D,avg}$) values were 68%, 62%, 52% and 45% for 0 vol%, 16 vol%, 32 vol%, and 48 vol%- porous PI films, respectively. For the optical scattering evaluation, the optical haze value which is defined as T_D (λ)/T_T (λ) is used. In Figure 4c, the calculated haze spectra also showed big differences between various porous polyimide layers, depending on the contents of DMAc. Although a porous PI from water had an average haze value of 0.88, the other calculated values were 0.77, 0.62 and 0.53 for the samples with 16 vol%, 32 vol%, and 48 vol%, respectively. In Figure 4d, one can easily notice that the order of optical clearance for a porous PI sample with different content of DMAc solvent was consistent with the trend in measured optical haze values. Based on these results, we can say that the optical scattering characteristic of a porous PI film can be controlled by changing the content of DMAc solvent in DIW non-solvent bath during the immersion precipitation process.

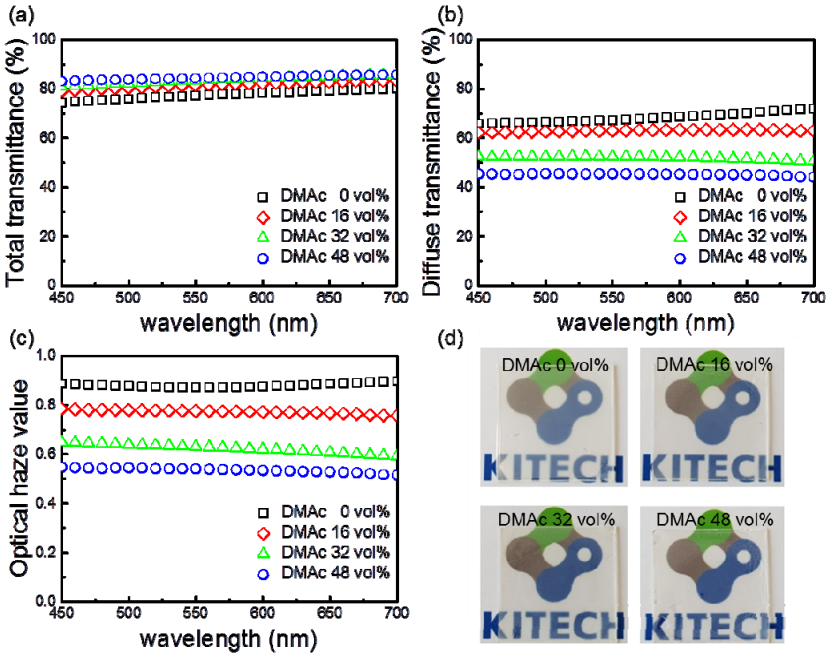

Figure 4. (a) measured total transmittance, (b) measured diffuse transmission, and (c) calculated haze spectra for the prepared porous polyimide scattering films on glass substrates using water bath with different contents of N,N-dimethylacetamide (DMAc) of 0 vol% (rectangular), 16 vol% (rhombus), 32 vol% (triangle), and 48 vol% (circle), (d) pictures of prepared porous scattering films on glass.

In the porous polymer materials, the light scattering happens at the interface between air and polymer matrix, basically. Then the scattering interface can exist not only at air voids inside the polymer media but also at the surface between polymer and ambient air. However, many previous researchers only focused on the roll of pores in the matrix, because the resultant surface was so flat enough to ignore the influence of the surface scattering [7–9,11]. And porous layer has been considered from the view point of stereology, as a two-phase random mixture of media material and air void [8,9]. Although those approaches have been introduced to understand their specific optical behaviors such as scattering elements depending on the shape of void or on the polarization of light, the demand on the simple but straightforward mechanism of optical scattering phenomena has increased for the practical application of the porous optical film. In this study, we correlated the resultant optical scattering characteristic with the micro-structure of a porous polymer layer, from the systematic analysis of both optical properties and micro-structures. To explain how the incident light scatters through the generated porous polymer layer, we proposed three scattering mechanisms illustrated in Figure 5.

As shown in previous section, the controls during pore-generation by immersion precipitation method accompanied with the change in the generated micro-structure of porous polymer films. At the condition with fast exchange rate, there were lots of air voids with large size over few micro-meter although the surface roughness was low. On the other hand, the number and size of the pores were reduced and the surface roughness was increased, when the contents of DMAc in DIW bath increased. To analyze the light scattering of particles, Mie approximation has been known to be

appropriate [18]. In Mie scattering theory, the power of light scattering is mainly governed by the size of particles. One can easily know that optical haze values in Figure 4c well matched to the estimated trend of light scattering by Mie scattering theory. The 0 vol%-sample had optical haze values of 0.88 because of light scattering at lots of air voids with size over 5 μm (Figure 5a).

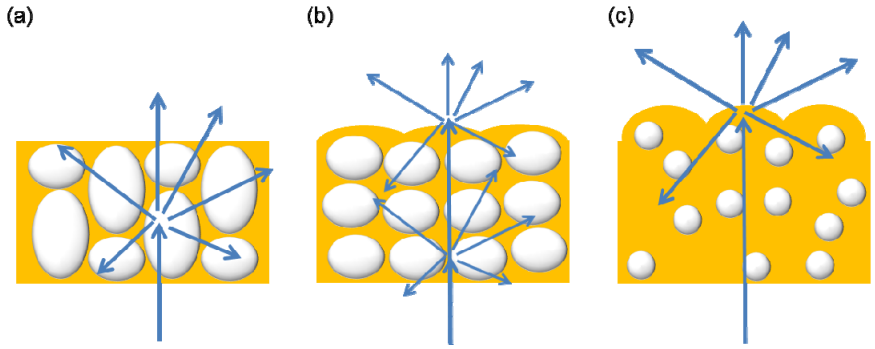

Figure 5. Schematic images of proposed optical scattering mechanisms in a porous polymer layer: (a) light scattering happens only inside pore-structure, (b) light scattering happens both inside pore-structure and at the rough surface, and (c) light scattering happens only at the rough surface.

However, it has to be noticed that the 48 vol%-sample still showed optical haze value of 0.53, in spite of a few pores were below 100 nm (see SEM images in Figure 2d). We stressed that the origin of optical haze of 48 vol%-sample mainly came from the light scattering at the rough surface (Figure 5c). When the light propagates through the interface between polymer material and air, the trace of rays can be influenced by the surface roughness. For a rough surface, Scalar surface scattering theory is known to be appropriate to check the influence of surface roughness on the optical scattering [19]. Based on Scalar surface scattering, the diffuse transmittance (T_D) can be accounted from the following equation:

$$T_D(\lambda) \cong T_T(\lambda) \times \left(1 - exp\left[-\left(2\pi\sigma_r \left| n_{polyimide}\, cos\,\theta_0 - n_{air}\, cos\,\theta_1 \right| / \lambda_{eff}\right)^2\right]\right) \quad (1)$$

where T_T is the total transmittance, σ_r is the surface roughness, and θ_0 and θ_1 are the angle of incidence and refraction of the specular beam. In Scalar scattering, light-scattering at the interfaces can be separated into a specular and a diffuse part. If the specular part is treated coherently throughout the structure similar with the measurement setup in Figure 4 (θ_0 equals to 0), one can easily check the influence of other parameters on the optical haze defined as $T_D(\lambda)/T_T(\lambda)$. As wavelength increases, the value of optical haze decreases. And the higher value of refractive index ($n_{polyimide}$) can introduce higher chance of optical scattering. However, the σ_r is the most significant parameter in surface scattering, because the variation of σ_r can be highest. From the Eq 1, the higher values of surface roughness make the higher values of optical haze. Based on our proposed light scattering mechanism, the optical haze values in 16 vol%- and 32 vol%-samples could be accounted from the light scattering both inside pore-structure and at the rough surface. The net power of light scattering could be expressed by the sum of Mie scattering and the surface scattering. In addition,

Mie scattering at air voids inside porous layer had more effects on the total amount of light scattering than the surface scattering at the rough surface.

4. Conclusion

This study investigated the systematic approach to explain the correlation between the generated micro-structure of a porous polymer layer and its optical scattering property. By changing the contents of DMAc solvent in water coagulation bath, the fine control of pore generation process using the immersion precipitation was possible. At the same time, the corresponding micro-structure of air voids in the resultant porous PI layer as well as its optical scattering characteristic can be also controlled. Then, we proposed the light scattering mechanism for a porous polymer film, which consists of air-voids inside the polymer media and the rough surface at the ambient interface. In addition, Mie scattering theory and Scalar surface scattering theory were introduced to account the light scattering inside pore structure and at the rough surface, respectively. Based on our systematic approach, it can be said that the net power of light scattering was the sum of Mie scattering and the surface scattering. In addition, Mie scattering influenced more on the total amount of light scattering more than the surface scattering. We expect that the work presented here will likely lay the foundation for fully understanding the scattering nature of porous polymer layer, which can be used to the conventional optics or optoelectronic devices

Acknowledgments

This study was conducted with the support of the Korea Institute of Industrial Technology, as "Development of the flexible luminescence-battery sheet based on high oxygen/moisture barrier films for the luminescent smart packaging (KITECH JA-18-0040)".

Conflict of interest

The authors declare there are no conflicts of interest in this paper.

References

1. Chang HW, Lee J, Hofmann S, et al. (2013) Nano-particle based scattering layers for optical efficiency enhancement of organic light-emitting diodes and organic solar cells. *J Appl Phys* 113: 204502-1–204502-8.
2. Song J, Kim KH, Kim E, et al. (2018) Lensfree OLEDs with over 50% external quantum efficiency via external scattering and horizontally oriented emitters. *Nat Commun* 9: 3207–3217.
3. Xue J, Gu Y, Shan Q, et al. (2017) Constructing Mie-Scattering Porous Interface-Fused Perovskite Films to Synergistically Boost Light Harvesting and Carrier Transport. *Angew Chem Int Ed* 56: 5232–5236.
4. Nirmal A, Kyaw AKK, Sun XW, et al. (2014) Microstructured porous ZnO thin film for increased light scattering and improved efficiency in inverted organic photovoltaics. *Opt Express* 22: A1412–A1421.

5. Hsu CW, Zhen B, Qiu W, et al. (2014) Transparent displays enabled by resonant nanoparticle scattering. *Nat Commun* 5: 3152–3158.
6. Kim E, Cho H, Kim K, et al. (2015) A Facile Route to Efficient, Low-Cost Flexible Organic Light-Emitting Diodes: Utilizing the High Refractive Index and Built-In Scattering Properties of Industrial-Grade PEN Substrates. *Adv Mater* 27: 1624–1631.
7. Bathelt R, Buchhauser D, Gärditz C, et al. (2007) Light extraction from OLEDs for lighting applications through light scattering. *Org Electron* 8: 293–299.
8. Malinka AV (2014) Light scattering in porous materials: Geometrical optics and stereological approach. *J Quant Spectrosc Ra* 141: 14–23.
9. Penttilä A, Lumme K (2009) The effect of the properties of porous media on light scattering. *J Quant Spectrosc Ra* 110: 1993–2001.
10. Koh TW, Spechler JA, Lee KM, et al. (2015) Enhanced outcoupling in organic light-emitting diodes via a high-index contrast scattering layer. *ACS Photonics* 2: 1366–1372.
11. Go H, Koh TW, Jung H, et al. (2017) Enhanced light-outcoupling in organic light-emitting diodes through a coated scattering layer based on porous polymer films. *Org Electron* 47: 117–125.
12. Strey R (1994) Microemulsion microstructure and interfacial curvature. *Colloid Polym Sci* 272: 1005−1019.
13. LEE KM, Fardel R, Zhao L, et al. (2017) Enhanced outcoupling in flexible organic light-emitting diodes on scattering polyimide substrates. *Org Electron* 51: 471−476.
14. Niesen B, Rand BP (2009) Thin Film Metal Nanocluster Light-Emitting Devices. *Adv Mater* 26: 1446–1449.
15. Kim YD, Kim JY, Lee HK, et al. (1999) Formation of polyurethane membrane by immersion precipitation. II. Morphology formation. *J Appl Polym Sci* 74: 2124–2132.
16. Reuvers AJ, van den Berg JWA, Smolders CA (1987) Formation of membranes by means of immersion precipitation: Part I. A model to describe mass transfer during immersion precipitation. *J Membrane Sci* 34: 45–65.
17. Reuvers AJ, van den Berg JWA, Smolders CA (1987) Formation of membranes by means of immersion precipitation: Part II. The mechanism of formation of membranes prepared from the system cellulose acetate-acetone-water. *J Membrane Sci* 34: 67–86.
18. Kelly K, Coronado E, Zhao L, et al. (2003) The Optical Properties of Metal Nanoparticles: The Influence of Size, Shape, and Dielectric Environment. *J Phys Chem B* 107: 668–677.
19. Zeman M, van Swaaij R, Metselaar JW, et al. (2000) Optical modeling of solar cells with rough interfaces: Effect of back contact and interface roughness. *J Appl Phys* 88: 6436–6443.

AIMS Press